EVS30 Symposium
Stuttgart, Germany, October 9 - 11, 2017

Prognosis of the remaining useful life of a Lithium Battery based on a data-driven method and Gaussian processes

Mikel Arrinda[1], Mikel Oyarbide[1], Haritz Macicior[1], Eñaut Muxika[2]

[1]*IK4-CIDETEC, Paseo Miramón 196, Donostia-San Sebastián 20014, moyarbide@cidetec.es*

[2]*Mondragon Unibertsitatea, Loramendi 4, Mondragón 20500*

Summary

One of the key factors for success automotive electrification is to predict the lifetime, understand the aging process and to prolong the operability of lithium ion battery. Therefore, this work presents the methodology and the main results obtained during the prognosis of remaining useful life of a Lithium Battery. This work combines extensive laboratory tests over the life time and the battery capacity variation estimation with a Gaussian Process (GP). Finally the suitability of the battery system under previously defined operation profile is evaluated using the dynamic model and the update capacity value for each aging state.

Keywords: Prediction, battery SoH (State of Health), battery model, cycle life, battery calendar life.

1 Introduction

Due to their outstanding properties, lithium ion batteries (LIBs) are one of the most used energy storage devices in different applications such as portable electronic devices, automotive and stationary. Electrochemical aging processes such as the increasing of Solid Electrolyte Interphase (SEI), loss of active materials, lithium plating, etc. are directly related to the loss of life and performance of a LIB. As a consequence of these aging mechanisms, the energy and power densities are reduced over the time until the batteries are not capable to satisfy application requirements. The prognosis of remaining useful life (RUL) is vital for ensuring the safety, long lifetime, predict system failure and even to generate new business models making use of such batteries in a second life. For this purpose, lifetime models describing the relation between system/component degradation and consumed lifetime have to be established accurately.

In order to make the RUL estimation of LIB, researchers have used different tools. Overall, those tools are divided in 2 main groups: methods based on mechanism analysis and methods based on data dining or data-driven analysis. In the same time, amongst the different methods based on data dining available in the literature, it is possible to make another classification of three main methods depending on the tools used for estimating the lifetime: artificial intelligence [1] [2], filtering [3] [4] [5] [6] and stochastic processes [4]. However, in many cases, studies have mixed several methods in order to strengthen each methods' weaknesses as in [3] [4].

The methods based on mechanism analysis observe the evolution of the physical mechanisms. The common ones explain the aging processes by the analysis of the electrochemical behaviour of the LIB in order to predict the lifetime. These methods are clear in physical significance and concepts [7] but they involve a lot of parameters and complex calculations for accurate modelling, so they are considered not suitable for real-time monitoring [8]. Another strategy found in the literature, taking into consideration the

aging models, considers two types of models: equivalent circuit based models [3] [9] and semi-empirical based models [10] which describe the aging evolution observed during experimentation. These models describe worse the evolution of the physical mechanisms but the complexity of the models decrease, making them suitable for implementation on board applications.

The methods based on data mining focus on extracting effective information about the LIBs' performance and constructing the degradation model to predict RUL from the available data sets. This way, inherent relationships and degradation trends based on the available data are established [7].

Methodologies using artificial intelligence usually process monitoring data to fit variables of the degradation model. It calculates the RUL by extrapolating the variables to the failure threshold [7]. In literature, there are many publications using autoregressive (AR) methods, neural networks (NN) [1] and relevance vector machines (RVM) [2] for implementing the prognosis. Each method has its strengths and weaknesses. Eddahech et al. [1] proposed a recurrent neural network (RNN) to predict the degradation in LIB performance. It proved that the neural network has a superior nonlinear approximation ability than the autoregressive methods, but at the same time, it requires a large amount of training data and it is likely to fall into a local minimum, which means having a wrong estimation [7].

In the same way, there are many analysis that use filtering methods based on Kalman filter [3] [5] [6], and particle filter [4]. Sepasi et al. [5] presented an online SoH and state of charge (SoC) estimation method for LIB packs using coulomb counting method to calculate SoC and the extended Kalman filter (EKF) to estimate SoH, which He et al. [6] used in order to compare EKF and Unscented Kalman Filter (UKF). According to the results, UKF provides higher accuracy than EKF, in the way Sepasi et al. [5] achieved the lifetime prognosis.

Several authors have used stochastic processes such as the Gaussian process regression (GPR) as Li et al. [4]. These methods capture the time-varying degradation process effectively by a statistical description of the degradation process. The degradation trends are learnt from battery data sets with the combination of Gaussian process functions. Stochastic methods are the ones which can better characterize the lithium battery degradation processes due to its accuracy according to Wu [7].

In this paper, a mixture of an equivalent circuit and a stochastic process method has been chosen as the RUL prognosis tool. This approach is based on the clearance in physical significance and concepts of the equivalent circuit and the high accuracy of predictions made by stochastic processes.

This paper is organized as follows: In chapter 2, the self-designed methodology to predict the aging and to evaluate the EOL of a battery is presented. Those fundamental components are: (1) the dynamic equivalent circuit model used to describe the dynamic behaviour of the battery. This model is used also to validate the fulfilment of the operation profile at the end of life (EoL) of the battery; (2) the aging model used to update the parameters of the dynamic model and used as prior knowledge in the stochastic tool (by laboratory testing); and (3) the stochastic tool itself used to make the estimation of the RUL, which in this case is a GP. In chapter 3, the results obtained with the proposed RUL prognosis tool are presented. In chapter 4 the discussion of the collected results is developed. Finally, the conclusions are drawn in chapter 5.

2 Methodology

The parameterization of the equivalent circuit is based on empirical data provided by the observation of extensive laboratory tests over the life time. Similarly, an aging model at different conditions is integrated as prior knowledge on a Gaussian stochastic method, in order to predict the capacity loss over unknown states and making the prognosis of lifetime estimation. The following flow chart (Figure 1) is implemented for predicting the battery lifetime.

1- Parametrization of the dynamic model using data from the previous characterisation tests.
2- Emulation of the battery behaviour considering operation conditions (application profile conditions).
3- Update of the battery parameter variation for next step time using the aging model and on board information. Storage of the parameter variation on a new data base.
4- Training of the Gaussian stochastic process using available data gathered on the previous steps.

5- Estimation of RUL, considering aging data and identifying at which status the battery system is not able to supply the power demand. Additional constraints such as voltage and temperature will be considered to respect other more restrictive limits that might be fixed by an external element such as power electronics or thermal management system.

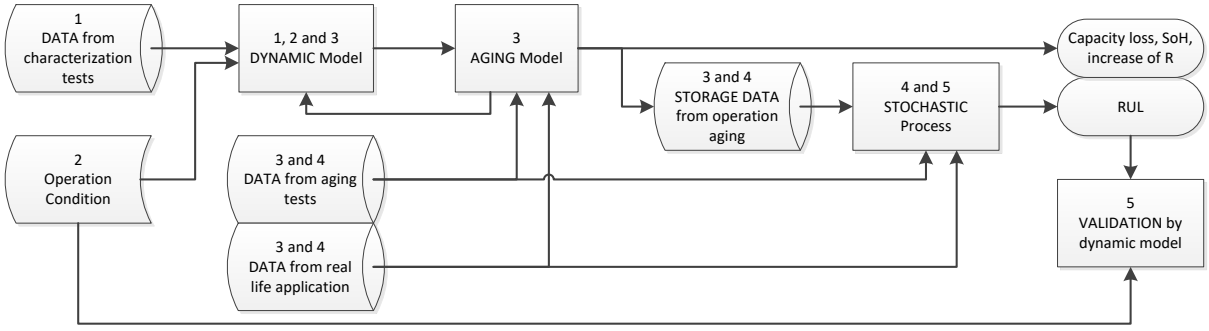

Figure 1: Defined flowchart to build the RUL of LIB.

In literature, end of life (EoL) criteria is commonly fixed when the capacity is decreased down to 80% or the impedance has risen to 200%, with respect to the initial value. However, even if the defined EoL is reached, the battery can still satisfy the application requirements depending on the sizing and the application power profile. Therefore, in this work the dynamic model integrated with the aging model is used to determine if the battery is still able to supply the power demand at each degradation status.

2.1 Dynamic equivalent circuit model

The degradation of LIBs is a nonlinear and time-varying dynamic electrochemical process [7]. Therefore, the RUL estimation model needs to represent accurately the dynamic behaviour of the cell under a real operation condition, in order to achieve an accurate consequence of the degradation. This work presents an electric equivalent circuit model (ECM) (see performance on Figure 2) based on a first order Randle equivalent circuit (eq. (1)) and a thermal equivalent circuit model (see performance on Figure 3) based on the sum of the joule and entropic heat (eq. (2)) that match the LIB dynamic performance.

$$V(t) = OCV - V_r(t) - V_{c1}(t) \tag{1}$$

$$Q_{total} = Q_{joule} + Q_{entropic} = I^2 R_{int} + IT\frac{\partial OCV}{\partial T} \tag{2}$$

The electric model is described by a space vector and a space state model (eq. (3), eq. (4) and eq. (5)) which are used as prior for the estimation of the posterior in a non-continuous domain.

$$\bar{x} = \begin{pmatrix} SoC \\ V_r \\ V_{c1} \end{pmatrix} \tag{3}$$

$$\begin{pmatrix} SoC \\ V_r \\ V_{c1} \end{pmatrix}_k = \begin{pmatrix} 1 & 0 & 0 \\ 0 & 0 & 0 \\ 0 & 0 & e^{\frac{-h}{R_1 C_1}} \end{pmatrix} \begin{pmatrix} SoC \\ V_r \\ V_{c1} \end{pmatrix}_{k-1} + \begin{pmatrix} \frac{-h}{36C_n} \\ R \\ R_1\left(1 - e^{\frac{-h}{R_1 C_1}}\right) \end{pmatrix} \mathrm{I_k} \tag{4}$$

$$V_k = \begin{pmatrix} 1 & -1 & -1 \end{pmatrix} \begin{pmatrix} OCV(SoC, T, \Psi) \\ V_r \\ V_{c1} \end{pmatrix}_k \tag{5}$$

As it can be observed in the state model shown in eq. (4) and eq. (5) the adopted system is 3rd order state vector with a dynamic matrix diagonal, namely consists of 1st order 3 different systems decoupled from each other. Similarly, the open circuit voltage (OCV) is obtained using a non-linear function (eq. (6)) which is dependent on the SoC, the temperature of the cell and the hysteresis characteristics imposed by the chemistry of the cell (Ψ) [11].

$$OCV = f(SOC, T, \Psi) \quad (6)$$

The thermal model is used to update the value of the inner temperature of the cell which is used in the OCV equation and in the resistance parametrization. The thermal equivalent circuit developed for this project is based on [12], whose description is out the scope of this paper.

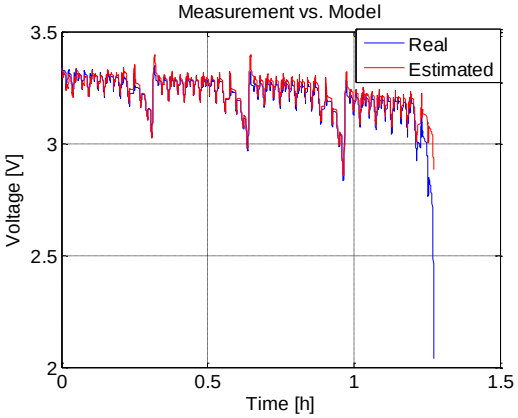

Figure 2: Electric model accuracy

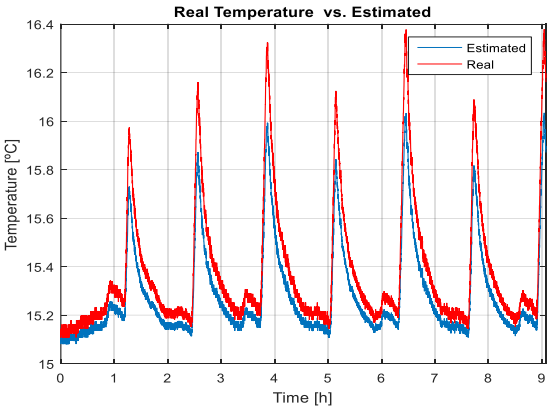

Figure 3: Thermal model accuracy.

2.2 Aging model

The chosen aging model is a semi-empirical one. Semi-Empirical Aging Models (SEAM) are generated using two different sources: extensive laboratory tests and on board applications. For the moment, it hasn't been used data collected from on board applications, but it is previewed to use this data in future lines. Anyway, using any of these information resources the relation between ageing accelerator factors (temperature, depth of discharge, current rate, SoC range) and aging indicators (typically capacity fade and impedance rise) is established. These aging indicators are coupled with the dynamic models, as stated, to determine if the battery is still able to supply the power demand.

In this case, aging behaviour of the battery (cycle and calendar life) is studied by the observation of extensive laboratory tests over the life time. The first test group will observe the degradation of the battery due to the cycling of the battery, while the calendar test will perceive the battery parameters variation due to the storage of the battery. In both cases, a predefined set of tests are conducted to evaluate the capacity fade and the impedance rise. This test matrix has been executed during more than a year, presenting a capacity fade higher than 20% in most cases.

Table 1: Designed test matrix to evaluate aging during cycling and calendaring.

	Cycling aging				Calendar aging	
	Temperature [ºC]	SoC ini[%]	DoD[%]	Current [C-rate]	Temperature [ºC]	SoC [%]
1	15	90	70	1	15	20
2	15	80	50	2	15	50
3	15	70	30	3	15	80
4	30	90	50	3	30	20
5	30	80	30	1	30	50
6	30	70	70	2	30	80
7	45	90	30	2	45	20
8	45	80	70	3	45	50
9	45	70	50	1	45	80

After evaluating the obtained results on the aging test matrix and in concordance with some authors [13] [14] [15], a linear aging model is taken where the aging stress factors in the cycling life and in the calendar life are taken separately into account (eq. (7)). The parameters of the model (α, β) have been optimized by a linear regression.

$$Q = Q_0 - Q_{cycling} - Q_{calendar} \quad (7)$$

The model that contains the effects of the cycling aging is described by a power law equation (eq. (8)) [16], were the power coefficient used is related to the different aging stress factors. The related stress factors are the maximum SoC that the battery reaches during the cycling, the depth of discharge (DoD), the ambient temperature (T) and the current rate (C-rate).

$$Q_{cycling} = Ah^{P_1} \tag{8}$$

The relationship between the capacity power coefficient (P_1) and the stress factors has been analysed empirically using polynomial and exponential expressions, selecting the best fitting of all tested cases in eq. (9) (see Figure 4), where the effect of the SoC and the DoD is described by second order polynomial equations (f_1 and f_2) and the C-rate and the T are taken into account by an exponential expression based on the Arrhenius equation.

$$P_1 = f_1(SoC) f_2(DoD) e^{\left(-\frac{\alpha_7 + \alpha_8 C_{rate}}{RT}\right)} \tag{9}$$

In the case of the calendar aging model, it has been also chosen a power law equation. However, in this case, in concordance to some authors [13], the decrease of the capacity is proportional to the root of the spent time in a steady state (the power of this equation is fixed to ½). The effect of the stress factors are related to the proportional coefficient (P_2) (eq. (10)).

$$Q_{calendar} = P_2 \sqrt{t} \tag{10}$$

The stress factors in this case are the SoC and the ambient temperature. Those 2 stress factors are described by exponential expressions based on the Arrhenius equation (eq. (11)) [16] (see Figure 5).

$$P_2 = \beta_1 e^{\left(-\frac{\beta_2}{SoC}\right)} e^{\left(-\frac{\beta_3}{RT}\right)} \tag{11}$$

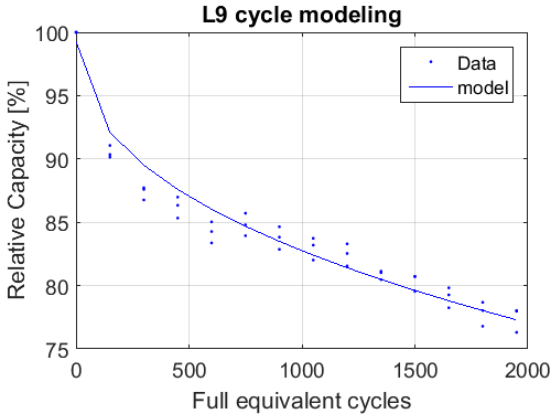

Figure 4: Fitted cycling aging model's α parameter using data of the 9º aging tests in Table 1.

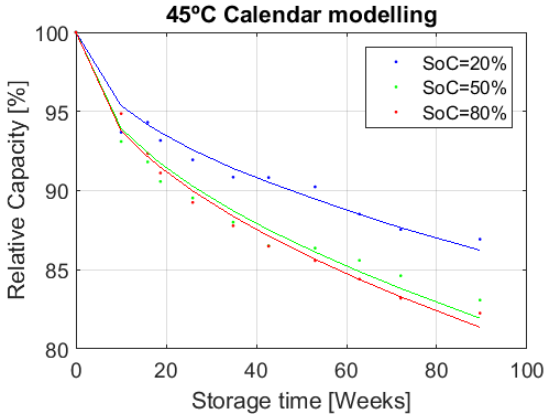

Figure 5: Fitted calendar aging model's β parameter using data of the 7º, 8º and 9º aging tests in Table 1.

2.3 Gaussian process for RUL prognosis

The prognosis of the RUL is carried out at battery level, where operational and environmental uncertainties take place due to unequal manufacturing or aging processes. Because of this, the tool which estimates the RUL needs to be flexible enough in order to take into account those uncertainties. Besides, at the same time, the tool needs to be robust enough against noises so as to give an appropriate RUL value. In this scenario, a GP is chosen to make the regression due to its ability and flexibility to provide uncertainty representation.

In a GP, observations occur in a continuous domain (time or space) and every point is associated with a normally distributed random variable. This supposes that every finite collection of those random variables has a multivariate normal distribution and that every finite linear combination of them is normally distributed. Supported by those assumptions, a GP defines a probability distribution over functions (eq. (12)) which is composed by a mean function and a covariance function (eq. (13) and eq. (14)).

$$f \sim GP\big(m(x), k(x,x')\big) \tag{12}$$

$$m(x) = E\big(f(x)\big) \tag{13}$$

$$k(x,x') = E\big[\big(f(x) - m(x)\big)\big(f(x') - m(x')\big)\big] \tag{14}$$

Typically a GP uses a mean function equal to zero with the aim of describing all the system by the covariance function since the covariance function is flexible enough to model the true mean arbitrary well [17]. However, having prior knowledge of the system, it is possible to express that prior information as the most probable result of the systems in form of the mean function, and then the GP is able to describe the uncertainties by the covariance function. In this case, a prior knowledge of the degradation taken from the SEAM has been used to define the mean function (eq. (7)) and a suitable covariance function (eq. (15)) has been chosen based on the results in [18]. According to Richardson et. al. [18] different covariance functions must be combined in lithium ion batteries RUL prognosis. The chosen combination of covariance functions is a mixed of a Squared Exponential (SE) covariance (eq. (16)) and a Matérn (Ma) covariance (eq. (17)) function.

$$k(x,x') = k_{SE}(x,x') + k_{Ma}(x,x') \tag{15}$$

$$k_{SE}(x,x') = {\sigma_{SE}}^2 exp^{\left(-\frac{1}{l^2}(x-x\prime)^2\right)} \tag{16}$$

$$k_{Ma}(x,x') = {\sigma_{Ma}}^2 \frac{2^{1-v}}{T(v)}\left(\sqrt{2v}\frac{(x-x\prime)}{\rho}\right)^v R_v\left(\sqrt{2v}\frac{(x-x\prime)}{\rho}\right) \tag{17}$$

Where the smoothness hyper-parameter v is taken as constant ($v = 3/2$) and the hyper-parameters σ_{SE}, σ_{Ma}, l and ρ are optimized using a training data set and the probability function of the Gaussian distribution.

The distribution over functions obtained by the GP is used as a prior for Bayesian inference. The calculated prior does not depend on the training data, but specifies some properties of the functions (the objective is to learn properties of the prior in the light of the training data) [17]. The calculation of the posterior will provide the predictions for unseen test cases. Again, we write out the joint distribution of everything we are interested in (eq. (18)) where the training set covariance (K), training-test set covariance (K_*) and the test set covariance (K_{**}) are calculated.

$$\begin{bmatrix} f \\ f_* \end{bmatrix} \sim \mathcal{N}\left(\begin{bmatrix} \mu \\ \mu_* \end{bmatrix}, \begin{bmatrix} \mathrm{K} & \mathrm{K}_* \\ \mathrm{K}_*^T & \mathrm{K}_{**} \end{bmatrix}\right) \tag{18}$$

Since we know the values for the training set f we are interested in, the conditional distribution of f_* given f can be expressed with eq. (19) (this is the posterior distribution for a specific set of unseen test cases). In the same way, the mean and the variance of the posterior can be deducted from here (see eq. (20) and eq. (21)).

$$f_* | f \sim N(\mu_* + \mathrm{K}_*^T K^{-1}(f - \mu), \mathrm{K}_{**} - \mathrm{K}_*^T K^{-1} K_*) \tag{19}$$

$$m_p(x) = m(x) + \mathrm{K}_*^T \mathrm{K}^{-1}(f - \mu) \tag{20}$$

$$k_p(x,x') = \mathrm{K}_{**} - \mathrm{K}_*^T \mathrm{K}^{-1} K_* \tag{21}$$

The estimation attained with this Bayesian inference is noiseless but it is something common to have noise in the observations of many applications of regression. In the Gaussian process models, such noise is easily taken into account. The easiest way of adding the noise effect in the observation is to assume that the noise is Gaussian and independent. In this scenario, the noise variance is added to the covariance values of each test point respect to the same test point ($k_p(x,x');\ x = x'$) (see eq. (22)). The equations of the posterior change to eq. (23) and eq. (24).

$$\mathrm{K}_y = K + \sigma_y I \tag{22}$$

$$m_p(x) = m(x) + \mathrm{K}_*^T {\mathrm{K}_y}^{-1}(f - \mu) \tag{23}$$

$$k_p(x,x') = \mathrm{K}_{**} - \mathrm{K}_*^T {\mathrm{K}_y}^{-1} K_* \tag{24}$$

In case there is available data from the real life application, and assuming that the capacity trends on the training and the real life application are correlated, the GP can take into account this new data as part of the training data in the estimation of the posterior as an extra input [19]. In the same way, this data will be also used to feed the current prior knowledge (SEAM) built using laboratory testing.

3 Results

The proposed method is tested firstly with the data of one aged cell from the static aging test matrix in order to check the data points that are needed for a precise RUL prediction using GP. The test results of test number 7 shown in Table 1 are selected to evaluate the performance of the GP under limited training data points. Then, data from the tested three cells under the same static aging test (number 7 shown in Table 1) is used where the data is compared to check the flexibility of the proposed prognosis tool under unit to unit uncertainties. Finally, a standard dynamic operation profile is proposed to be tested with the aim of evaluating the EoL criteria (Figure 8). Thanks to the proposed prognosis model, the state of health of the battery can be estimated in the exact moment that the battery doesn't fulfil the requirements of the dynamic profile. The safe operation window of the battery is fully used under the operation profile in this state.

The optimized parameters used on the covariance functions on the evaluations are shown in Table 2.

Table 2: Optimized hyper-parameters of the covariance function

	σ_{SE}	ρ	σ_{Ma}	l
Static aging test	5	1000	9	10000
Dynamic aging test	5	1000	9	10000

In the first evaluation, the relation between the amount of the data used for training and the performance of the estimation is evaluated. For this, the data set defined for training has been collected in an increasing 1/8 range from the whole available data set (see Figure 6).

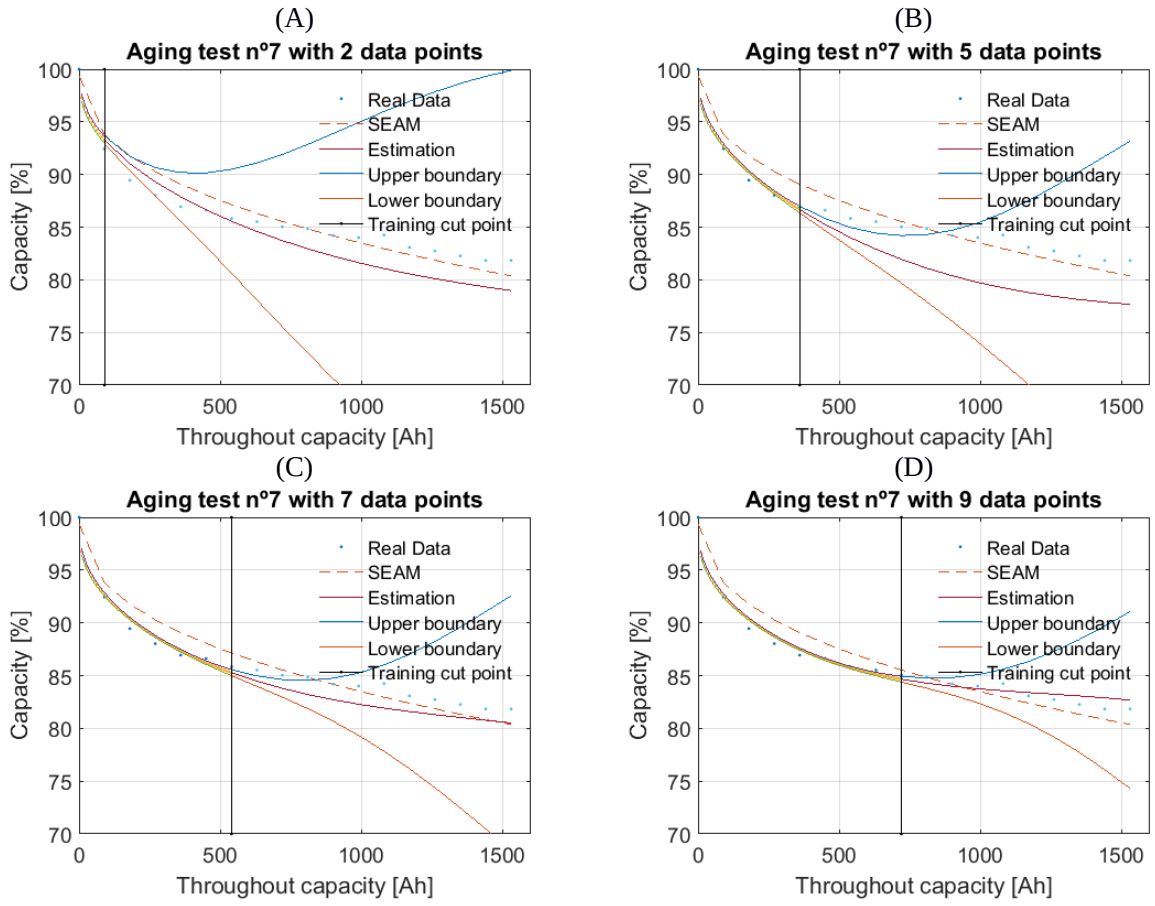

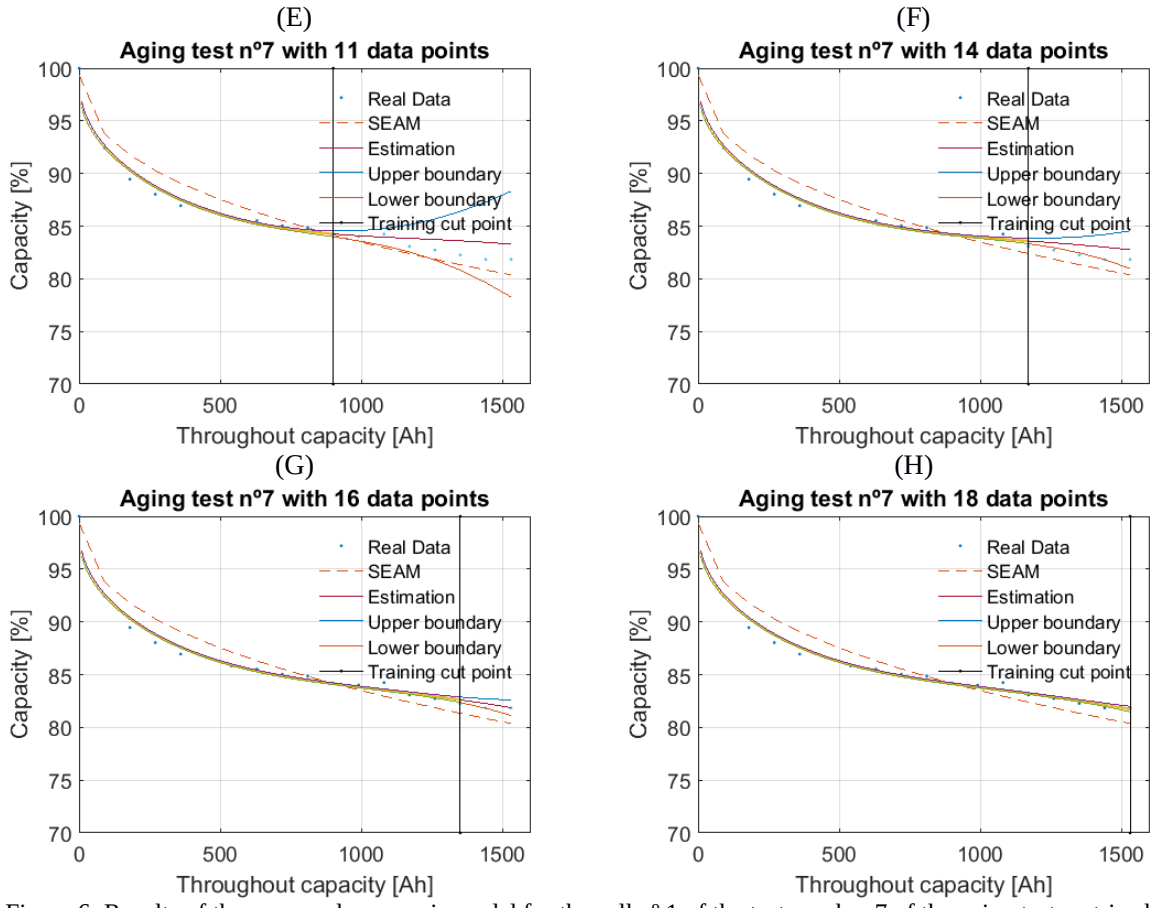

Figure 6: Results of the proposed prognosis model for the cell nº 1 of the test number 7 of the aging test matrix shown in Table 1. The training data set has been modified form A to H in a 1/8 range, where (A) has been evaluated with a 1/8 of the available data (2 data points) and H with a 8/8 (18 data points).

The obtained result varying the amount of training data points has been evaluated using 2 different indicators that are shown in Table 3. The first indicator being evaluated is the mean square error between all the available data and the estimated values using the GP in both sets (in the training set and in the test set). The second indicator is the error of the estimation done respect to the last test data point. As a reference, it has been added the indicators achieved with the SEAM alone fitted to the whole data set.

Table 3: Indicators of the results obtained changing the amount of training data of the GP

	First indicator	Second indicator
2 data points (A in Figure 6)	0.4759	2.8594
5 data points (B in Figure 6)	0.7664	4.1780
7 data points (C in Figure 6)	0.3368	1.3279
9 data points (F in Figure 6)	0.2275	0.8439
11 data points (E in Figure 6)	0.2562	1.4442
14 data points (F in Figure 6)	0.2320	0.9176
16 data points (G in Figure 6)	0.2131	0.0263
18 data points (H in Figure 6)	0.2125	0.1120
Aging model (Dashed line in Figure 6)	0.2993	1.4786

In the second evaluation, the flexibility of the chosen prognosis tool is evaluated, using data from the rest of the batteries used in the test number 7 of the test matrix proposed in the aging model (Table 1). For this aim, it has been used a training set containing the ¾ of the whole data set (the first battery is the picture F in Figure 6 and the other two batteries are shown in Figure 7).

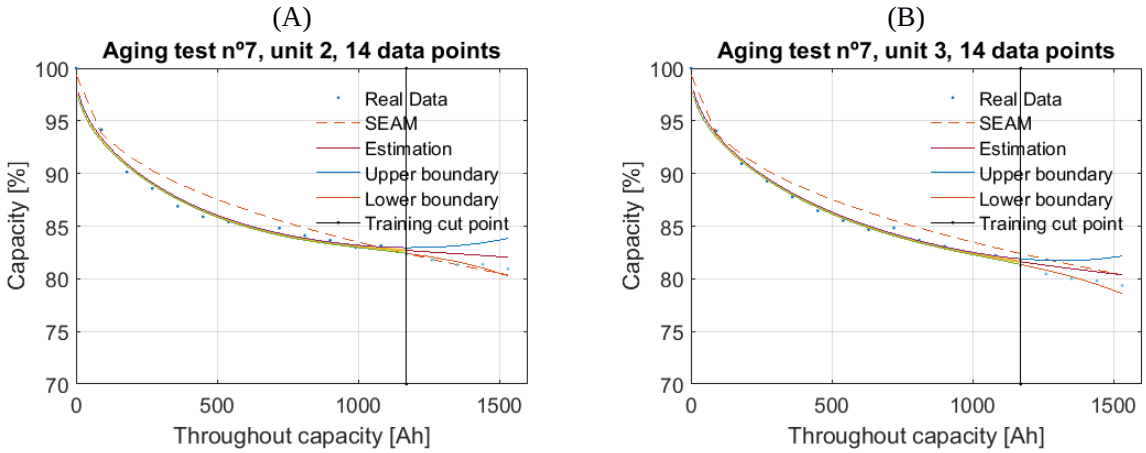

Figure 7: Results of the proposed prognosis model for the cell nº 2 (A) and nº 3 (B) of the test number 7 of the aging test matrix shown in Table 1. The used training data set has been a ¾ or 6/8 of the available data (14 data points).

The indicators used to check the flexibility of the chosen prognosis tool are placed in Table 4. The first indicator being evaluated is the mean square error between all the available data and the estimated values using the GP in both sets (in the training set and in the test set). The second indicator is the error of the estimation done respect to the last test data point. As a reference, it has been added the indicators achieved with the SEAM alone fitted to the whole data set for each of the 3 cell units.

Table 4: Indicators of the results obtained with a ¾ training data set on 3 cells under the same aging test.

	First indicator	Second indicator
Cell unit 1 (F in Figure 6)	0.2320	0.9176
Cell unit 2 (A in Figure 7)	0.2064	1.1037
Cell unit 3 (B in Figure 7)	0.1790	1.0078
Aging model in the 3 units	[0.2993, 0.2665, 0.2685]	[1.4786, 0.5807, 1.0078]

In the third evaluation, a standard dynamic operation profile called “New European Driving Cycle” (NEDC) is applied cyclically (Figure 8Figure 1). Along the lifetime, the NEDC is applied at each aging state to the dynamic model in order to evaluate when the battery is not able to supply the demand of the four urban driving cycles (UDC) of the NEDC and consequently, to identify the EoL of the battery. The EoL will be reached when the NEDC comprises the whole operation window of the aged cell. Thanks to this, the fulfilment of the requirements imposed to the battery by the application is checked.

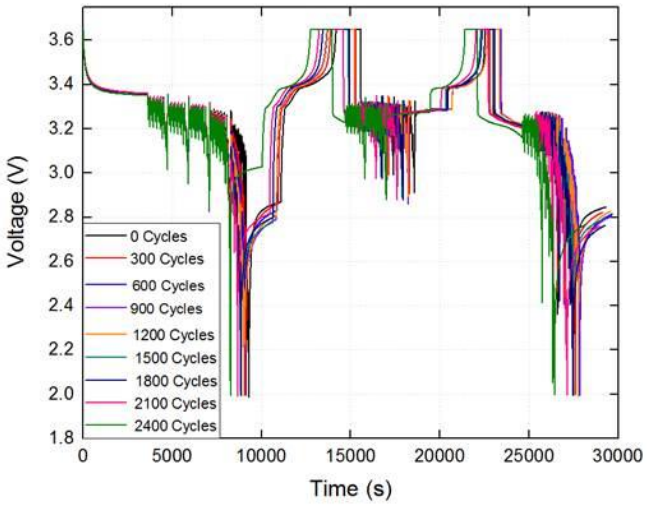

Figure 8: Dynamic operation profile in different aged state of the tested cell.

The results are shown in Table 5. In this case, the capacity is the variable used to define the EoL since the R has increased hardly anything.

Table 5: Results obtained from the validation step of the RUL prognosis tool.

	Cycles	Capacity
Fresh state	0	100
EoL	2400	85.69

4 Discussion

In this paper, the potential of the proposed RUL prognosis method is evaluated from three different points of views. The first one has taken into account the required amount of data points for reliable estimation, the second one has compared (the unit to unit uncertainties) the estimations done on three different samples and the third one has reviewed the EoL criteria.

In the first evaluation, data from 1 cell aged under a static aging test has been chosen to check the amount of data points needed for a precise RUL estimation. The results in Table 3 show that the best situation should be taking into account all the 18 available data points in the data set. In the same way, it can be seen that the GP of the prognosis tool, taking as reference the results obtained with 18 data points using only the SEAM, is able to improve the estimation of the unknown states with only 9 training data points (a half of the whole data set). However, the results also show a trend change in the error of the estimated RUL when the training data is increased from 9 to 11 data points. In this case, the errors are equal to the ones obtained by the SEAM alone. This trend change in the error can be caused by a change of the trend on the capacity fade behaviour or due to a bad measurement during the experimentation. Explanations about the change of the trend on the capacity fade due to a change on the predominant degradation mechanisms are developed in the literature. The fact of having more than one degradation mechanism responsible for the aging carries on a difficulty in the identification of the interesting trend and would require enlarging the training data set. By the other hand, the data points 10 and 11 could have been measured wrongly, which could have leaded the GP to learn a not correct trend which would lead to incorrect estimation. The solution should come from an improvement on the measurement equipment and methodology. This last situation of having wrong measurements could mean that the trend learnt until 9 data points is correct and that thanks to the GP it would be possible to reduce the needed data set to the half in order to have the same results as with only using the SEAM.

In the second evaluation, it has been chosen data from 3 cells aged under the same static aging test to check the precision and flexibility of the proposed prognosis tool. The results of the 3 units (Table 4) show that the prior knowledge based on the aging model can be fitted with a mean square error less than 0.3% and with an error in the last tested value less than 1.5%. However, better results can be achieved thanks to the GP. The results on the first unit (Table 3) show that thanks to the GP, a better fitting and estimation can be achieved with the same amount of training data since the estimation error is reduced from 1.4% to 0.1% and the fitting mean square error is reduced from 0.29% to 0.21%. At the same time, the results of the 3 units (Table 4) show that even with less training data points, better or at least more reliable results can be obtained thanks to the GP. The estimation with the SEAM is done with an error which goes from a 1.5% to a 0.6%. The GP, whereas makes the estimation with an error which goes from 1.1% to 0.9% making use of 14 data points instead of 18.

Finally, a dynamic operation profile has been chosen so as to test the last part of the prognosis tool: the validation of the dynamic performance of the battery at the EoL. In this case, the battery has not been able to fulfil the requirements of the operation profile of four UDCs at an early aged state. The results show that the EoL is reached before the conventional 80% respect to the nominal capacity of the cell having unchanged the internal resistance. This fact shows that the not fulfilment of the operation profile of the defined application of the battery can come earlier than the expected one.

5 Conclusions

In this paper, a RUL prognosis tool is presented which is composed by an electro-thermal equivalent circuit model (ECM), a semi-empirical aging model (SEAM) and a stochastic estimation tool based on a Gaussian

Process (GP). To make the RUL prognosis, i) the ECM firstly describes the dynamic behaviour of the battery in a continuous time domain. ii) The SEAM describes the most probable evolution of the parameters of the battery in the course of the battery life. iii) The GP estimates unknown estates based on the prior knowledge while dealing with uncertainties and iv) finally, the ECM checks the fulfilment of the operation profile, to decide technically the End of life of the battery.

According to the Results obtained in chapter 3, it can be concluded that:

- The estimations are improved extending the amount of data inputs in the training set.
- Thanks to the GP is possible to obtain better results with less data points.
- The quality of the data is an important asset.
- The estimations made by a SEAM are improved adding a GP. In the 3 cases on the second evaluation, the GP is able to give an estimated value with a similar error, showing the high flexibility and the high precision of the estimation done by the GP against unit to unit uncertainties.
- The definition of the EoL criteria should not be taken as a constant and instead of that, it should be taken as a parameter of the prognosis tool.

References

[1] A. Eddahech, O. Briat, N. Bertrand, J.-Y. Delétage, and J.-M. Vinassa, "Behavior and state-of-health monitoring of Li-ion batteries using impedance spectroscopy and recurrent neural networks," *Int. J. Electr. Power Energy Syst.*, vol. 42, no. 1, pp. 487–494, 2012.

[2] D. Wang, Q. Miao, and M. Pecht, "Prognostics of lithium-ion batteries based on relevance vectors and a conditional three-parameter capacity degradation model," *J. Power Sources*, vol. 239, pp. 253–264, 2013.

[3] S. Sepasi, R. Ghorbani, and B. Y. Liaw, "A novel on-board state-of-charge estimation method for aged Li-ion batteries based on model adaptive extended Kalman filter," *J. Power Sources*, vol. 245, pp. 337–344, 2014.

[4] F. Li and J. Xu, "A new prognostics method for state of health estimation of lithium-ion batteries based on a mixture of Gaussian process models and particle filter," *Microelectron. Reliab.*, vol. 55, no. 7, pp. 1035–1045, 2015.

[5] S. Sepasi, R. Ghorbani, and B. Y. Liaw, "Inline state of health estimation of lithium-ion batteries using state of charge calculation," *J. Power Sources*, vol. 299, pp. 246–254, 2015.

[6] W. He, N. Williard, C. Chen, and M. Pecht, "State of charge estimation for electric vehicle batteries using unscented kalman filtering," *Microelectron. Reliab.*, vol. 53, no. 6, pp. 840–847, 2013.

[7] L. Wu, X. Fu, and Y. Guan, "Review of the Remaining Useful Life Prognostics of Vehicle Lithium-Ion Batteries Using Data-Driven Methodologies," *Appl. Sci.*, vol. 6, no. 6, p. 166, 2016.

[8] C. Lin, A. Tang, and W. Wang, "A Review of SOH Estimation Methods in Lithium-ion Batteries for Electric Vehicle Applications," *Energy Procedia*, vol. 75, pp. 1920–1925, Aug. 2015.

[9] Z. Guo, X. Qiu, G. Hou, B. Y. Liaw, and C. Zhang, "State of health estimation for lithium ion batteries based on charging curves," *J. Power Sources*, vol. 249, pp. 457–462, 2014.

[10] J. Wang *et al.*, "Cycle-life model for graphite-LiFePO4 cells," *J. Power Sources*, vol. 196, no. 8, pp. 3942–3948, 2011.

[11] M. Oyarbide, "Energy storage systems based on electrochemical devices," mondragon unibertsitatea, 2012.

[12] G. Vertiz-Navarro, "Gestión térmica de sistemas de almacenamiento de energía basados en baterías litio-ion," Mondragon Unibertsitatea, 2015.

[13] E. Sarasketa-Zabala, E. Martinez-Laserna, M. Berecibar, I. Gandiaga, L. M. Rodriguez-Martinez, and I. Villarreal, "Realistic lifetime prediction approach for Li-ion batteries," *Appl. Energy*, vol. 162, pp. 839–852, 2016.

[14] B. Xu, "Degradation-limiting Optimization of Battery Energy Storage Systems Operation," *Power Syst. Lab. ETH Zurich*, no. September 2013, 2013.

[15] A. Hoke, A. Brissette, A. Pratt, and K. Smith, "Electric Vehicle Charge Optimization Including Effects of Lithium-Ion Battery Degradation," 2011.

[16] L. a. Escobar and W. Q. Meeker, “A Review of Accelerated Test Models,” *Stat. Sci.*, vol. 21, no. 4, pp. 552–577, 2007.

[17] C. E. Rasmussen, “Gaussian processes for machine learning,” *Int. J. Neural Syst.*, vol. 14, no. 2, pp. 69–106, 2006.

[18] R. R. Richardson, M. A. Osborne, and D. A. Howey, “Gaussian process regression for forecasting battery state of health,” 2017.

[19] M. Osborne, “Bayesian Gaussian Processes for Sequential Prediction, Optimisation and Quadrature,” *Quadrature*, p. 234, 2010.

Authors

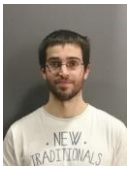

Mikel Arrinda received the University degree in industrial electronic engineering in 2012. In 2013 completed his studies with Master’s degree in integration of renewable energy sources into the electricity grid. After three years of activity in a private company, in 2017, he joined IK4-CIDETEC to develop a methodology to make prognosis of the RUL of lithium ion batteries.

Mikel Oyarbide received the B.S. degree in automatic and industrial electronic engineering in 2009. Since then, he joined to IK4-CIDETEC working in the field of Battery management systems. In 2013 he obtained Phd degree in SoC and SoH estimator algorithms, from the University of Mondragon. His current research interests are on the design, development and validation of battery packs.

Haritz Macicior received the M.Sc. degree in electric engineering at École Polytechnique de Montrèal (EPM) in 2004. Since 2005 he works in IK4-CIDETEC. Currently is the Head of Energy Storage Systems Unit. His present research interests are the development of battery management system (BMS, modelling, SoC/SoH/SoF algorithms) and smart grids.

Eñaut Muxika Olasagasti is a lecturer and a researcher at Mondragon Unibertsitatea and he obtained his PhD in Electrical Engineering from the Institute National Polytechnique de Grenoble (INPG) in 2002. He has worked in machine-tool and power electronics control systems. His current research interests include reliability, availability, safety and performance modelling, model-based system engineering and adaptive hardware, software, communication system design.